IOPscience iopscience.iop.org

Home Search Collections Journals About Contact us My IOPscience

Ab initio phonon dynamics of iridium

This article has been downloaded from IOPscience. Please scroll down to see the full text article.

1998 J. Phys.: Condens. Matter 10 7967

(http://iopscience.iop.org/0953-8984/10/36/007)

View the table of contents for this issue, or go to the journal homepage for more

Download details:
IP Address: 171.66.16.209
The article was downloaded on 14/05/2010 at 16:43

Please note that terms and conditions apply.

J. Phys.: Condens. Matter **10** (1998) 7967–7973. Printed in the UK PII: S0953-8984(98)93215-5

Ab initio phonon dynamics of iridium

R Heid†, K-P Bohnen‡, K Felix‡, K M Ho§ and W Reichardt‡

† Max-Planck-Institut für Physik komplexer Systeme, Nöthnitzer Straße 38, D-01187 Dresden, Germany

‡ Forschungszentrum Karlsruhe, Institut für Nukleare Festkörperphysik, PO Box 3640, D-76021 Karlsruhe, Germany

§ Ames Laboratory, US Department of Energy and Department of Physics, Iowa State University, Ames, IA 50011, USA

Received 7 April 1998, in final form 29 June 1998

Abstract. We present an investigation of the phonon spectrum of the transition metal iridium within the framework of a *first-principles* pseudopotential mixed-basis method. The full phonon spectrum is determined by means of a real-space approach, which involves only supercell force calculations. Pronounced anomalies are predicted for the [110] direction, which are similar to the ones observed for rhodium. First results of an inelastic neutron scattering investigation of the phonon dispersions are in very good agreement with the *ab initio* calculations and confirm the predicted anomalies. We present all interatomic force constants up to the 12th-nearest-neighbour shell obtained by a least-squares fit to supercell force constants of four different supercells. Theoretical phonon densities of states and elastic constants are compared with experimental data.

1. Introduction

Anomalies in phonon spectra indicate peculiarities of lattice interactions, which are often linked to specific features of the electronic structure. A well known example of this linkage is provided by the transition metals, for which inelastic neutron scattering experiments have provided a rather complete picture of anomalous dispersion relations, which have their origin in the presence of d states at the Fermi surface. Because of their large absorption cross sections for thermal neutrons, rhodium and iridium represent two noticeable exceptions, whose phonon spectra have not been accessible until recently. In the case of rhodium, pronounced anomalies along high-symmetry phonon branches of Rh, especially along the [110] direction, have been predicted by an *ab initio* electronic structure calculation, and have been subsequently confirmed by neutron scattering experiments [1]. Because the fifth-row element iridium possesses an electronic structure very similar to that of Rh, one may expect it to exhibit phonon anomalies of similar type. So far, only a small number of transverse frequencies have been published; these are not sufficient to identify or exclude anomalous features of the phonon dispersions [2].

As a reciprocal-space approach, density functional perturbation theory provides [3, 4] a natural way to study phonon anomalies from *first principles*, and has been successfully applied to a number of transition metals [5]. On the other hand, standard direct-space approaches (frozen-phonon/supercell methods) generally require very large unit cells to properly cope with the long range of the lattice interaction implied by the dispersion anomalies. In previous work [6], we have demonstrated that this difficulty can be avoided

0953-8984/98/367967+07$19.50 © 1998 IOP Publishing Ltd

by combining results obtained from various calculations with supercells of different sizes and symmetries. In an application to Rh, we have determined a set of real-space force constants, which allowed us to carry out a sufficiently accurate interpolation of the whole phonon spectrum, including the observed anomalies.

In this paper, we apply this scheme to the transition metal Ir; as far as we are aware, this represents the first *ab initio* investigation of its phonon spectrum. Our calculations are based on a mixed-basis pseudopotential formulation in the local density approximation to density functional theory. They predict pronounced dips in [110] branches similar to but even stronger than the ones observed for Rh. First results of a current neutron scattering experiment nicely support the theoretical findings. We determine interatomic force constants up to the 12th NN (where NN stands for nearest neighbour), and compare the phonon density of states and elastic properties derived with available experimental data. Our results are in disagreement with previous predictions based on pseudopotential perturbation theory [2, 7, 8]. Similar discrepancies exist in the case of Rh, emphasizing the need for accurate *ab initio* electronic structure calculations for establishing a quantitative description of the lattice dynamics in transition metals.

The paper is organized as follows. In the next section, we briefly outline the technical details of the applied method. The results for Ir are presented in section 3, which is followed by a summary.

2. Method

We have performed *first-principles* electronic structure calculations for Ir using a pseudopotential approach within the framework of density functional theory. The local density functional approximation with the Hedin–Lundqvist parametrization for the exchange and correlation potential has been employed throughout [9]. The frozen core of Ir is represented by a relativistic norm-conserving pseudopotential of Hamann–Schlüter–Chiang type [10], whose details are described in reference [11]. Electronic wave functions are represented by a mixed-basis set which consists of plane waves up to a kinetic energy of 10.0 Ryd and five localized orbitals of d symmetry obtained from atomic 5d pseudo-orbitals smoothly cut off at a radius of 2.55 Å. A Gaussian broadening width of 0.02 eV has been applied in the k-point sampling. The theoretical lattice constant (3.85 Å) and bulk modulus (3.88 Mbar) are in good accord with the experimental values of 3.84 Å [12] and 3.66 Mbar [13], respectively.

Our approach to the lattice dynamics aims at determining a set of interatomic force constants (IFCs) which is complete enough to allow an accurate description of phonon dispersions to be given for the whole Brillouin zone (BZ). Because the method has already been described in some detail in reference [6], we will just sketch the main ideas in the following.

Total-energy or force calculations performed for distorted atomic configurations within a fixed supercell geometry provide access to supercell force constants (SFCs), such as planar force constants in the case of a supercell stretched along a high-symmetry direction of the crystal. Because of the periodic boundary conditions implied by the supercell, the SFCs are given as linear combinations of the IFCs. Therefore, IFCs cannot be derived directly from a single supercell, unless the size of the supercell is big enough to extend beyond the range of the lattice interaction. This limitation can be overcome by combining the results for SFCs obtained for several supercells to obtain a large set of linear equations for the IFCs, which are then 'inverted' to give the IFCs by means of a least-squares fit. Provided that the supercell geometries have been chosen properly, this method can also be applied to cases where the lattice interaction extends well beyond the size of each individual supercell.

Because the coefficients entering the linear equations for the IFCs only depend on the supercell geometries, systematic searches for favourable combinations can be carried out before performing any actual *ab initio* calculation. The efficiency of this approach has been demonstrated for Rh, where the interaction range extends beyond the ninth neighbour [6].

For the present study of Ir, we have adopted the same supercells as for Rh. They consist of three supercells stretched along the [100], [110], and [111] directions, respectively, each with 18 atomic layers. This set is augmented by a low-symmetry supercell containing 26 atoms (with basis vectors (1 0 5), (−5 0 1), (1 −2 1) in units of half the lattice constant). All of the calculations are based on the theoretical lattice constant, and the k-meshes used for the BZ integration correspond approximately to a mesh of 70 k-points in the irreducible wedge of the BZ of the underlying fcc lattice. We have extracted supercell force constants by performing force calculations for geometries with the central atom displaced by 0.02 Å. To increase the numerical accuracy, residual forces for the undistorted supercell geometry are subtracted, and the resulting forces are corrected for anharmonic contributions [14].

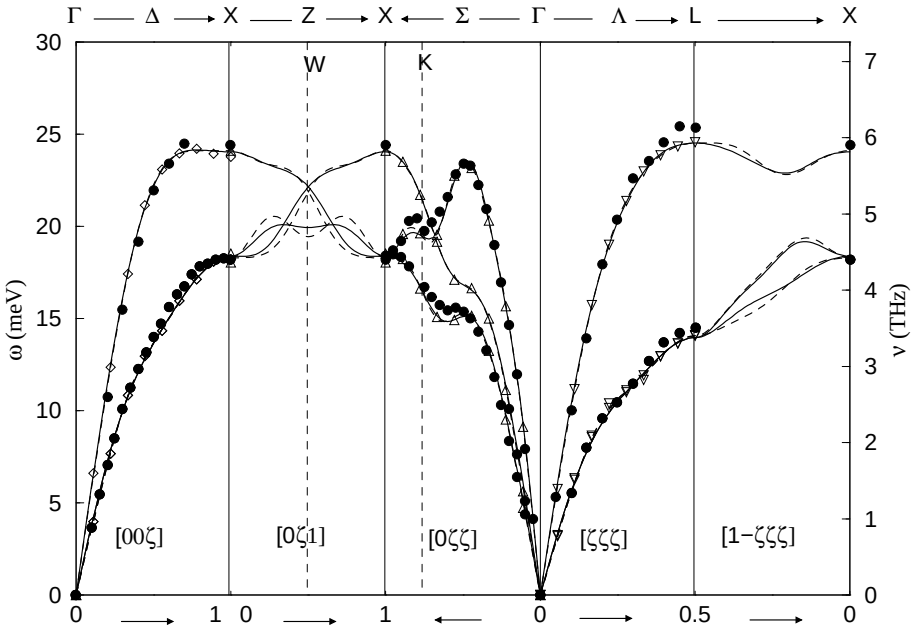

Figure 1. Phonon dispersions of iridium along various high-symmetry directions. The solid and dashed lines represent the theoretical results for the 12th-NN and 16th-NN fit, respectively. The open symbols denote frequencies derived directly from individual supercells. Experimental data are shown as filled circles.

3. Results

The theoretical results for the phonon dispersions of Ir are summarized in figure 1 for various high-symmetry directions of the fcc Brillouin zone. The open symbols indicate frequencies of phonon modes which are derived directly from calculations involving a single supercell stretched along a symmetry direction of the lattice. These calculations predict strong anomalies in all branches along [110], as well as shallow dips in the TA branches along [100] and [111]. While the form and position of

these anomalies are very similar to those of the ones observed for Rh [1, 6], the anomalies are more pronounced, especially for the lower TA branch along [110], where our calculations even suggest a negative dispersion in the vicinity of $\zeta = 0.6$. Another characteristic feature is the flattening of the LA [100] branch towards the X point.

Investigations of the phonon spectrum of Ir by inelastic neutron scattering face severe experimental difficulties because of the large absorption cross section of Ir, which leads to an unfavourable signal-to-background ratio and a fast increase of the induced radioactivity. So far, only a few transverse phonon frequencies along [100] and [110] have been reported by Ivanov *et al* [2]. Currently, inelastic neutron scattering experiments are being performed at the Orphee reactor at Saclay to obtain a more complete account of the phonon dispersions of Ir. First results of this investigation are shown as filled circles in figure 1 (room temperature data) [15]. Complementary measurements for the largely missing TA branch along [110] and along the boundary of the Brillouin zone are currently planned for the near future and will be reported elsewhere [16]. The available data agree very nicely with the *ab initio* calculation and confirm the existence of anomalies at the predicted positions.

Table 1. Interatomic force constants (in 10^3 dyn cm^{-1}) up to the 12th-nearest-neighbour shell for two fits taking into account all force constants up to the 12th- and 16th-nearest-neighbour shells.

NN	Index	Components			12th NN			16th NN		
0	000	xx			−254.78			−255.11		
1	110	xx	zz	xy	22.18	−2.04	24.71	22.18	−2.08	24.67
2	200	xx	yy		12.15	−5.49		12.35	−5.47	
3	211	xx	yy	xz	3.08	2.38	1.85	3.38	2.44	1.64
		yz			−1.05			−1.41		
4	220	xx	zz	xy	1.98	−0.24	1.25	1.97	−0.65	2.04
5	310	xx	yy	zz	1.08	0.01	0.40	0.88	−0.20	0.61
		xy			0.07			0.03		
6	222	xx	xy		0.90	0.64		0.59	0.54	
7	321	xx	yy	zz	−1.44	0.05	−0.90	−1.34	0.15	−1.00
		xy	xz	yz	−0.48	−1.20	−0.44	−0.27	−1.27	−0.26
8	400	xx	yy		−0.90	−1.49		−1.37	−1.20	
9	411	xx	yy	xy	−0.73	0.54	0.23	−0.84	0.62	−0.07
		yz			−0.03			−0.14		
9′	330	xx	zz	xy	3.18	0.54	2.99	3.22	0.92	3.73
10	420	xx	yy	zz	−0.28	0.21	−0.33	0.01	0.30	−0.33
		xy			0.08			0.00		
11	332	xx	zz	xy	−0.39	0.15	−0.17	−0.38	0.68	−0.46
		xz			0.02			0.29		
12	422	xx	yy	xy	1.08	−0.01	0.18	1.32	−0.08	0.00
		yz			0.11			0.24		

As described in the previous section, interatomic force constants can be derived by combining results from the high-symmetry supercells with those for the low-symmetry supercell containing 26 atoms using a least-squares-fit procedure. Because of the rather long range of the lattice interaction, as is evident from the anomalous features in the phonon spectrum, a large cut-off radius for the IFCs must be chosen. We present results for two fits which include all IFCs up to the 12th- and 16th-nearest-neighbour shells. Table 1 contains

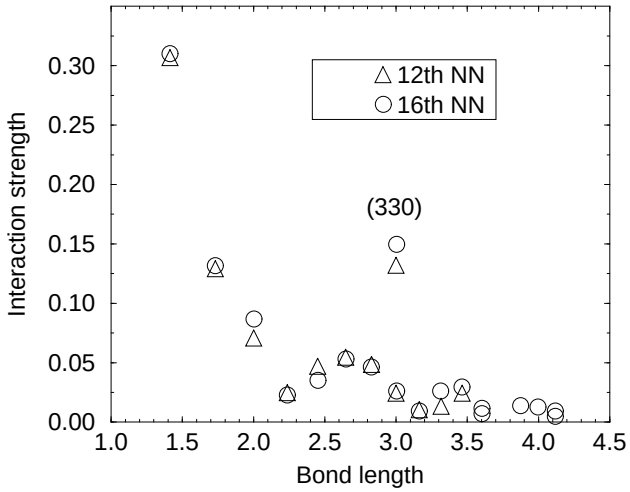

Figure 2. The average interaction strength of a shell as a function of the shell radius. Both axes are normalized to the values of the first-neighbour shell. Triangles and circles denote results for the 12th-NN and 16th-NN fit, respectively.

the corresponding values for the IFCs up to the 12th shell. Because the average

$$I(b) = \sqrt{\frac{1}{3}\sum_{\alpha\beta}\Phi_{\alpha\beta}^2(b)} \tag{1}$$

where $\Phi_{\alpha\beta}(b)$ denotes the force constant matrix assigned to a bond b, has the same value for each bond belonging to the same shell, it can be taken as a measure of the average interaction strength of a shell. A plot of I as a function of the shell radius is shown in figure 2. Its most prominent feature is the large value obtained for the (3 3 0) shell, whose average interaction strength is two to three times larger than those for all other

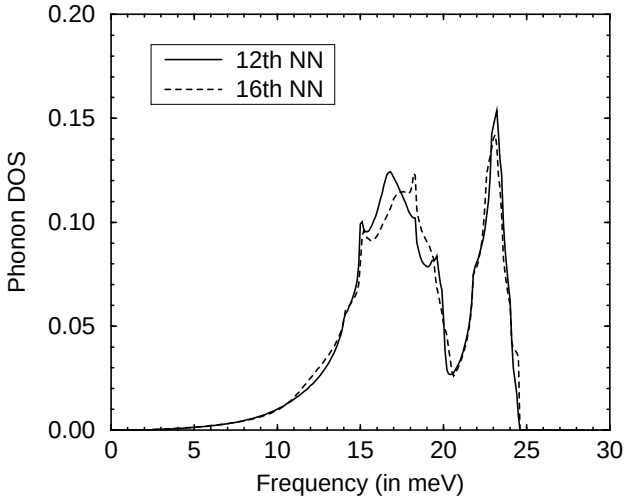

Figure 3. The calculated phonon density of states of iridium for 12th-NN and 16th-NN fits.

shells beyond the fourth neighbours. For larger distances, IFCs decay rapidly, and they are negligible beyond the 12th NN. A similar behaviour has been found for Rh [6].

Phonon dispersions derived from fitted IFCs are shown in figure 1, and the corresponding phonon density of states in figure 3. The characteristic structures of the latter agree well with those of point-contact spectra, which possess peak structures at 17.5 meV and 23 meV, and a cut-off frequency of 26 meV [17]. The dependence of the theoretical results on the chosen cut-off is small but more pronounced than for Rh, which indicates a larger effective range of the lattice interaction.

Table 2. Elastic constants and bulk moduli in units of 10^{12} dyn cm^{-2}. $C' = (C_{11} - C_{12})/2$ is related to the slope of the lower [110] branch at Γ. The experimental values are taken from reference [13].

	C_{11}	C_{12}	C_{44}	C'	B
12th-NN fit	6.97	2.69	2.94	2.14	4.12
16th-NN fit	6.67	2.82	2.55	1.93	4.11
Total energy	6.10	2.77	2.84	1.67	3.88
Experiment	5.96	2.52	2.70	1.72	3.66

As a further test for the derived IFCs, we have calculated the elastic constants via the method of long waves, which relates the elastic constants to sums over force constants weighted by the bond vector [18]. A second access is provided by the method of homogeneous deformations, where elastic properties are derived from changes in the total energy under homogeneous deformations of the unit cell. Table 2 compares our results for the elastic constants as obtained with the two methods to experimental values [13]. The values derived from the total-energy calculations are in reasonable agreement with experiment (less than 7% difference), while those based on IFCs show larger deviations (up to 16%) and a higher sensitivity to the chosen cut-off. This is also reflected in the failure of the 16th-NN fit to reproduce the negative Cauchy pressure ($C_{12} < C_{44}$) observed for Ir. The limited accuracy of the method of long waves is related to the fact that force constants contribute with a weight proportional to the square of the shell radius. Therefore, the elastic constants depend sensitively on small changes of the IFCs for distant shells.

In the present calculation, as well as in the previous investigation of Rh [1], relativistic effects are taken into account for the construction of the pseudopotential, while valence electrons are treated non-relativistically. Spin–orbit coupling is known to be important for a proper description of the electronic structure of Rh and Ir, where, for the latter, typical coupling strengths are larger by a factor of three than for Rh [19]. However, the good agreement between the calculation and experiment as regards the phonon dispersions of the two metals, including the positions and strengths of the anomalies, suggests that spin–orbit coupling does not significantly affect the lattice dynamical properties in these cases.

Our results for the lattice dynamics of Ir clearly disagree with previous theoretical investigations based on pseudopotential perturbation theory [2, 7, 8]. In this approach, the phonon spectrum is obtained in second-order perturbation theory on the basis of a model pseudopotential, whose parameters are determined from fits to static properties of the crystal. All proposed pseudopotential models for Ir predict cut-off frequencies substantially higher ($>10\%$) than our results; this can be traced back to the absence of a pronounced flattening of the branches in the vicinity of the BZ boundary. Furthermore, the [110] anomaly is either absent [2, 8] or is predicted to occur at much smaller wave vectors ($\zeta = 0.25$) [7]. Thus, pseudopotential perturbation theory, while often adequate for describing lattice properties of

simple metals, seems to be unable to capture the specific features of the phonon spectrum of the transition metal Ir.

4. Summary

We have presented an *ab initio* analysis of the lattice dynamics of iridium within a pseudopotential mixed-basis approach. Interatomic force constants up to the 12th NN are derived via a supercell technique, and indicate an important contribution to the lattice interaction from the 9th-NN shell. The phonon spectrum of Ir bears many similarities to those of the isoelectronic metal Rh. It exhibits anomalies in several high-symmetry branches at similar positions to but with larger amplitudes than those for Rh. Recent neutron scattering experiments for the [100], [110], and [111] directions nicely confirm our theoretical dispersion relations. The phonon spectrum as well as elastic properties are in satisfactory agreement with available experimental data.

References

[1] Eichler A, Bohnen K-P, Reichardt W and Hafner J 1998 *Phys. Rev.* B **57** 324
[2] Ivanov A S, Katsnelson M I, Mikhin A G, Osetskii Yu N, Rumyantsev A Yu, Trefilov A V, Shamanaev Yu F and Yakovenkova L I 1994 *Phil. Mag.* B **69** 1183
[3] Baroni S, Giannozzi P and Testa A 1987 *Phys. Rev. Lett.* **58** 1861
[4] For a recent review, see
Gonze X 1997 *Phys. Rev.* B **55** 10 337 and references therein
[5] Savrasov S Y and Savrasov D Y 1996 *Phys. Rev.* B **54** 16 487
de Gironcoli S 1995 *Phys. Rev.* B **51** 6773
Bungaro C, de Gironcoli S and Baroni S 1996 *Phys. Rev. Lett.* **77** 2491
[6] Heid R, Bohnen K-P and Ho K M 1998 *Phys. Rev.* B **57** 7407
[7] Antonov V N, Milman V Yu, Nemoshkalenko V V and Zhalko-Titarenko A V 1990 *Z. Phys.* B **79** 223
[8] Katsnelson M I, Naumov I I, Trefilov A V, Khlopkin M N and Khromov K Yu 1997 *Phil. Mag.* B **75** 389
[9] Hedin L and Lundqvist B I 1971 *J. Phys. C: Solid State Phys.* **4** 2064
[10] Hamann D R, Schlüter M and Chiang C 1979 *Phys. Rev. Lett.* **43** 1494
Bachelet G B, Hamann D R and Schlüter M 1982 *Phys. Rev.* B **26** 4199
[11] Elsässer C, Takeuchi N, Ho K M, Chan C T, Braun P and Fähnle M 1990 *J. Phys.: Condens. Matter* **2** 4371
[12] Ashcroft N W and Mermin N D 1976 *Solid State Physics* (Orlando, FL: Saunders College Publishing)
[13] MacFarlane R E, Rayne J A and Jones C K 1966 *Phys. Lett.* **20** 234
[14] Ho K M, Fu C L and Harmon B N 1983 *Phys. Rev.* B **28** 6687
[15] The data published in reference [2] are consistent with the present experiment for the [100] direction, but deviate significantly for the [110] direction.
[16] Reichardt W 1998 to be published
[17] Khotkevich A V 1996 *Physica* B **218** 31
[18] Born M and Huang K 1954 *Dynamical Theory of Crystal Lattices* (Oxford: Oxford University Press)
[19] Andersen O K 1970 *Phys. Rev.* B **2** 883